

“Structural and Functional Comparisons of Nucleotide Pyrophosphatase/

Phosphodiesterase and Alkaline Phosphatase: Implications for Mechanism and Evolution.”

Jesse G. Zalatan, Timothy D. Fenn, Axel T. Brunger, and Daniel Herschlag

Departments of Chemistry, Biochemistry, Molecular and Cellular Physiology, Neurology and Neurological Sciences, Stanford Synchrotron Radiation Laboratory, and the Howard Hughes Medical Institute, Stanford University, Stanford, California 94305

Figure S1. Identical inhibition of diesterase and monoesterase activities. Inhibition of NPP-catalyzed MpNPP¹⁻ hydrolysis (□) and pNPP²⁻ hydrolysis (○) by tungstate (A) and GMP (B). Activity was normalized by the observed rate constant in the absence of inhibitor. The lines are nonlinear least-squares fits for competitive inhibition and give K_i values of 149 ± 7 and 166 ± 16 μM for tungstate inhibition of diesterase and monoesterase activities, respectively, and K_i values of 298 ± 22 and 259 ± 22 μM for GMP inhibition of diesterase and monoesterase activities, respectively.

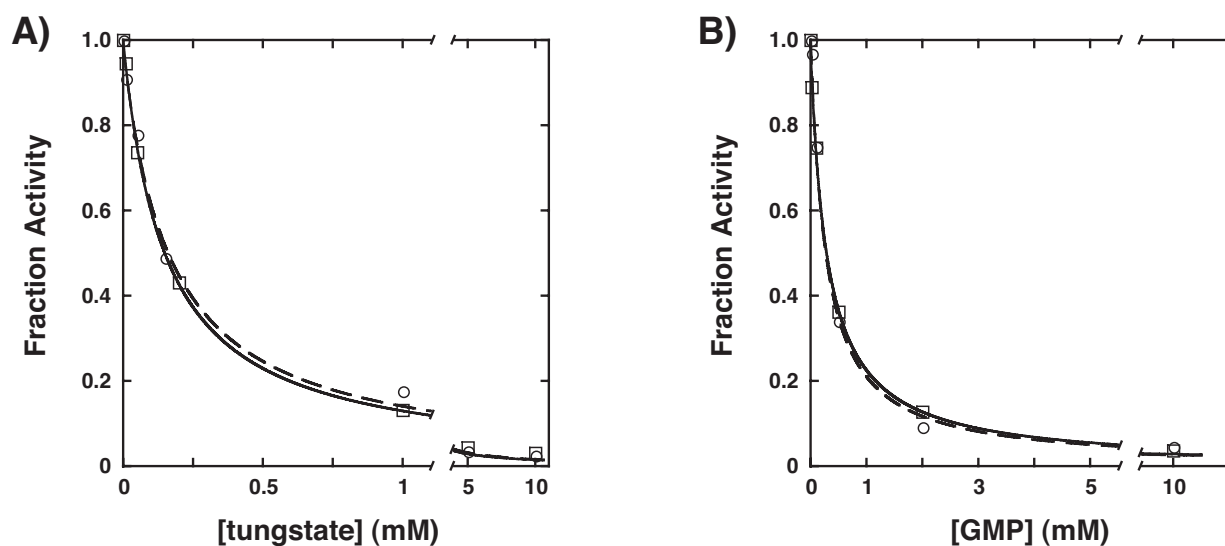


Figure S2. Experimentally Phased Map of the NPP Active Site. Experimental phases were obtained from a three wavelength MAD dataset at the Zn edge. The Zn^{2+} ions (green) were placed with SOLVE (S1). The map shown was generated from phases derived from density modification using RESOLVE (S2). All Zn^{2+} ligands are clearly resolved and the quality of the experimental maps allowed for building of 95% of the protein chain.

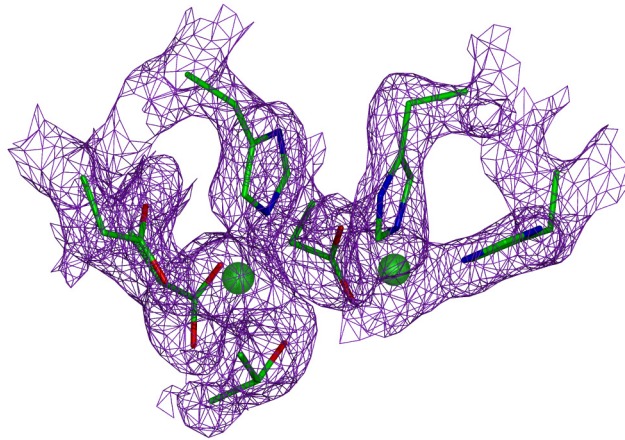
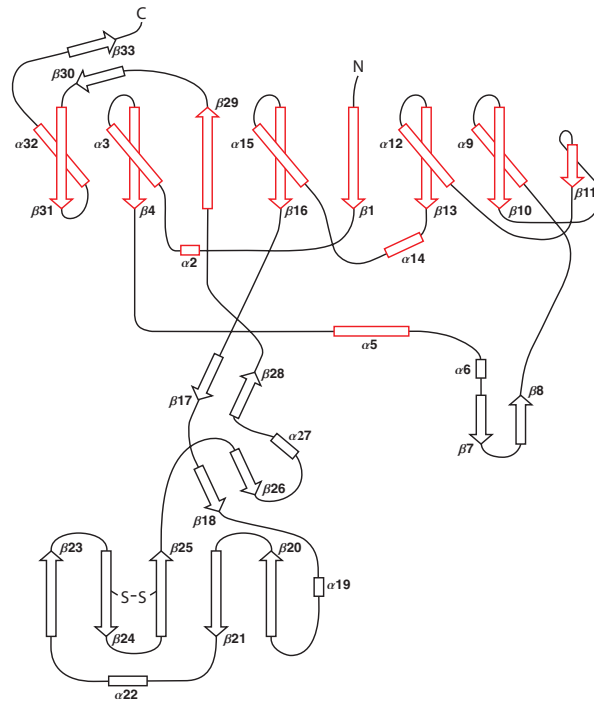


Figure S3. Topology diagrams of the secondary structures of NPP (A) and AP (B). Secondary structure elements are shown in red in both diagrams if any part of the secondary structures are aligned in the three dimensional structures. The topology of the linkages between aligned secondary structure elements is conserved between the two structures, consistent with divergent evolution from a common ancestral sequence.

A) NPP



B) AP

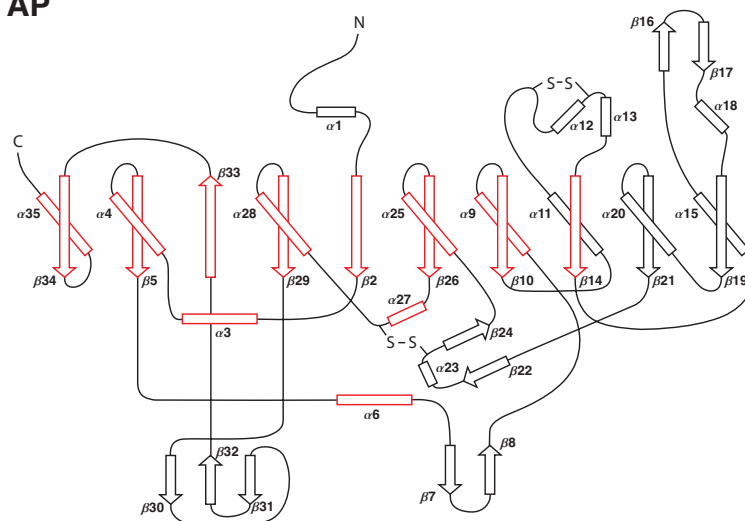


Figure S4. Structure-based sequence alignments of NPP and AP. An initial sequence alignment based on the structural alignment (see main text Figure 5) was generated with Swiss-PdbViewer (S3) and manually corrected by inspection of the aligned structures. Residues in uppercase correspond to stretches of sequence that align between the two structures. Residues in lowercase correspond to stretches of sequence that do not align between the two structures, and the placement of these residues in the sequence alignment is somewhat arbitrary. Residues are marked as identical (*) or similar (: or .) only in the regions of aligned structure (uppercase). Similar pairs are those with positive scores in the PAM 250 matrix (S4), and are marked ":" for scores >0.5 or "." for scores ≤0.5, following the Clustalw alignment format (S5). The percent structural homology is 52%, calculated with respect to the length of the shortest sequence (NPP, 382 residues). The percentages of identity and similarity (including identity) in the structurally homologous regions are 16% and 50%, respectively. The active site Ser or Thr nucleophile and the conserved Zn²⁺ ligands are highlighted in green. Secondary structure elements for each sequence are annotated using the notation from Figure S3.

```

Xac NPP      44      -----tpHALLLISIDGLRADMLD-
E. coli AP   1      tpempvlenraaaggditapggarrltgdqtaalrdsldkpaKNIILLIGMGMDSEITa
                                     : : : : * : . :
                                     α1      β2      α3

                                     α3      β4      α5      α6
Xac NPP      63      -----rgitpNLSHLareGVRARWMAPSY-----PSLTFPNHYTLVTGLRPd
E. coli AP   61      arnyaegaggffkGIDAL---PLTG-QYTHYAlnkktgkpdvTDSAASATAWSTGVKT-
                                     . : . * : . : : : : * : : :
                                     α4      β5      α6

                                     β7      β8      α9      β10
Xac NPP      105     hhgivhnsrmdptlggfwlsksevlgdarwggEPVWVGVENTGQHAATWswpgseaa--
E. coli AP   116     -----yngalgvdihekdhPTILEMAKAAGLATGNVstaelqdatp
                                     . : . : * : . :
                                     β7      β8      α9      β10      α11

                                     β11
Xac NPP      163     -----ikgvrpSQWRh-----
E. coli AP   157     aalvahvtsrkcygpsatsekcpgnalekkgkgsiteqllnaraDVTlGggaktfaetat
                                     .
                                     α12      α13      β14      α15      β16

Xac NPP      174     -----yqkgvrl-----
E. coli AP   217     agewgqkltreqaqargyqlvsdaaslnsvteanqqkpllgfадgnmpvrwlgpkatyh

                                     β17      α18      β19      α20      β21      β22
Xac NPP      181     -----dTRVDAVRGWLATDGA-QRNRLVTLYFEHVLEAGHDHGPE
E. coli AP   277     gnidkpvavtctpnprndsvpTLAQMTDKAIELLSKkEKGFFLQVEGASIKQDLAANPC
                                     * . : . : . : : : : * : . * .
                                     α23      β24      α25      β26      α27

                                     α15      β16      β17      β18      α19
Xac NPP      220     SrqYADAVRAVDAAIGRLLAGMQRDGtraRTNIIIVSDHGMAEvapghaisvediappqi
E. coli AP   337     G--QIGETVDLDEAVQRALEFAKKEG---NTLVIVTADHHAHAsqivapdtkapglqtaln
                                     . . : * * : * * : : * . * : * : * * .
                                     α28      β29      β30      β31

                                     β20      β21      α22      β23      β24      β25
Xac NPP      280     ataitdgqvigfeplpggqaaaeasvlgahdhycwrkaelparwqygshpriplvcqm
E. coli AP   392     t-----

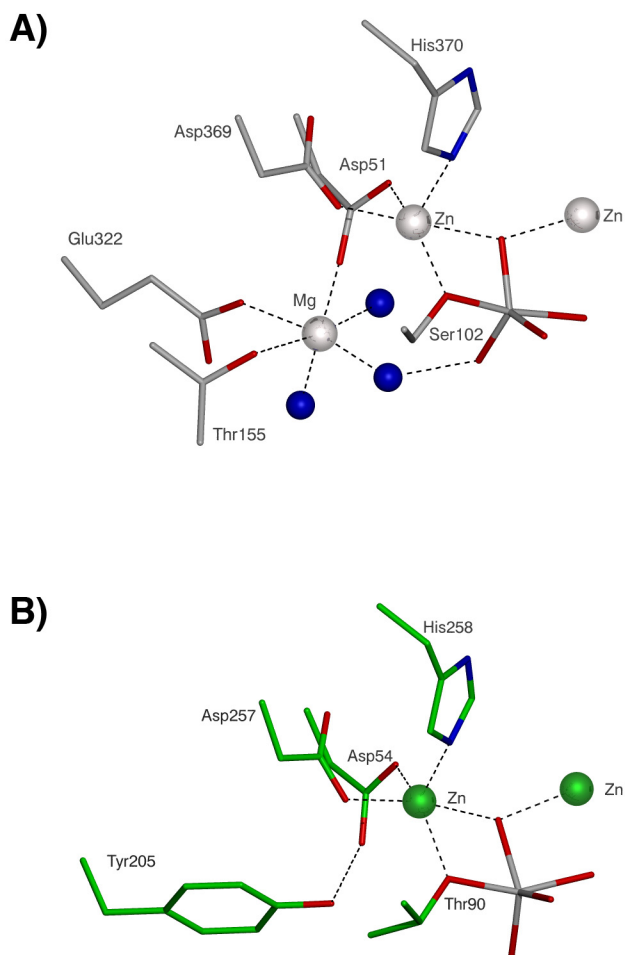
                                     β26      α27      β28      β29      β30      β31      α32
Xac NPP      340     hegwdalfpdklakraqrgtRGSFGYDpalpsmRAVFLAQGPDLaqgkltlPGFDNVVDVYA
E. coli AP   393     ---kdgavmvmsygnseedsSQEHTGS-----QLRIAAYGPHA--anvvGLTDQTDLFY
                                     . * . : : * * . : * : : :
                                     β32      β33      β34      α35

                                     β31
Xac NPP      400     LMSRLLGIPAAPNDGNPATLLPALRM-----
E. coli AP   441     TMKAALGLK-----
                                     * . * :

```

Alignment Statistics	(# of residues)/(total aligned)	Percentage
Structural Homology	199/382	52
Identity (overall)	31/382	8
Identity (homologous region)	31/199	16
Similarity (homologous region)	100/199	50

Figure S5. Comparison of the Mg^{2+} site of AP (S6) with the corresponding region of NPP in structures with vanadate bound in the active site. A) The Mg^{2+} site in AP. Thr155, Glu322, Asp51, and three water molecules (blue spheres) coordinate Mg^{2+} in an octahedral geometry. Asp51 is also a Zn^{2+} ligand (see main text Figure 8). One of the Mg^{2+} -bound water molecules is positioned to contact an equatorial oxygen atom in the vanadate ligand. B) The corresponding region of NPP. Tyr205 occupies the region corresponding to the Mg^{2+} site in NPP and forms a hydrogen bond with Asp54. Asp54 is a Zn^{2+} ligand in NPP and corresponds to Asp51 in AP.



References

- (S1) Terwilliger, T. C., and Berendzen, J. (1999) Automated MAD and MIR structure solution. *Acta Cryst. D55*, 849-861.
- (S2) Terwilliger, T. C. (2000) Maximum-likelihood density modification. *Acta Cryst. D56*, 965-972.
- (S3) Guex, N., and Peitsch, M. C. (1997) SWISS-MODEL and the Swiss-PdbViewer: An environment for comparative protein modeling. *Electrophoresis 18*, 2714-2723.
- (S4) Gonnet, G. H., Cohen, M. A., and Benner, S. A. (1992) Exhaustive matching of the entire protein sequence database. *Science 256*, 1443-1445.
- (S5) Thompson, J. D., Higgins, D. G., and Gibson, T. J. (1994) Clustal W: improving the sensitivity of progressive multiple sequence alignment through sequence weighting, position-specific gap penalties and weight matrix choice. *Nucleic Acids Res. 22*, 4673-4680.
- (S6) Holtz, K. M., Stec, B., and Kantrowitz, E. R. (1999) A model of the transition state in the alkaline phosphatase reaction. *J. Biol. Chem. 274*, 8351-8354.